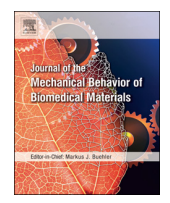


Contents lists available at ScienceDirect

## Journal of the Mechanical Behavior of Biomedical Materials

journal homepage: www.elsevier.com/locate/jmbbm



## Durability of Poly(3,4-ethylenedioxythiophene) (PEDOT) films on metallic substrates for bioelectronics and the dominant role of relative shear strength



Jing Qu<sup>a,1</sup>, Nikolay Garabedian<sup>b</sup>, David L. Burris<sup>b,c</sup>, David C. Martin<sup>a,c,\*</sup>

- <sup>a</sup> Materials Science and Engineering, The University of Delaware, Newark, DE, 19716, USA
- <sup>b</sup> Mechanical Engineering, The University of Delaware, Newark, DE, 19716, USA
- <sup>c</sup> Biomedical Engineering, The University of Delaware, Newark, DE, 19716, USA

#### ARTICLE INFO

# Keywords: Adhesion Relative shear strength Durability poly(3,4-ethylenedioxythiophene) Bioelectronic materials

#### ABSTRACT

Despite growing interest in the use of conducting polymer coatings such as poly(3,4-ethylenedioxythiophene) (PEDOT) in bioelectronics, their relatively poor mechanical durability on inorganic substrates has limited long-term and clinical applications. Efforts to enhance durability have been limited by the lack of quantifiable metrics that can be used to evaluate the polymer film integrity and associated device failure. Here we examine the hypothesis that film failure under the tribological and cyclic electrical stressing becomes substantially less likely when the interfacial shear strength ( $\tau_i$ ) exceeds the shear strength of the film ( $\tau_f$ ). In this paper, we: (1) develop a simple yet robust method to quantify the relative shear strength ( $\tau_i$ / $\tau_f$ ); (2) quantify the effect of substrate and surface treatment on the relative shear strength of PEDOT; (3) relate changes in relative shear strength to resistance to interface failure under cyclic electrical and tribological testing. Treating a stainless-steel substrate with an adhesion promoter increased  $\tau_i/\tau_f$  from 0.18 to 0.69 compared to untreated controls. On untreated gold, the  $\tau_i/\tau_f$  of PEDOT increased to 1.46. Whereas both cyclic electrical and tribological testing quickly and severely damaged the interface of PEDOT when  $\tau_i/\tau_f < 1$ , neither stimulus had any quantifiable effect on delamination when  $\tau_i/\tau_f > 1$ .

#### 1. Introduction

Organic bioelectronics have become increasingly attractive in recent years for use in seamless electronic-biological interfaces (Forrest, 2004) (Berggren and Richter-Dahlfors, 2007) (Savagatrup et al., 2014a) (Someya et al., 2016). An important trend is the replacement of hard, inorganic conductors or semiconductors with softer, conducting polymers at the interface between the device and the biological tissue. It has been found that the impedances of conducting polymers at biologically significant frequencies (1-1000 Hz) are substantially lower, and charge storage capacities are larger than typical metals and metal oxides including indium-tin-oxide (ITO) (Nyberg et al., 2007), iridium oxide (IrOx) (Wilks et al., 2009) (Boehler et al., 2016), gold (Leleux et al., 2014), platinum (Boehler et al., 2016) (Venkatraman et al., 2011), and platinum-iridium (Bodart et al., 2019). This results in superior signalto-noise ratios (Sessolo et al., 2013) and lower voltages during stimulation (Chen et al., 2017). With lower density and stiffness, conducting polymers also have the potential to be superior material candidates from the perspective of mechanical biocompatibility with living tissues (Lee et al., 2005) (Lind et al., 2013). The advantage of conducting polymers has been demonstrated in cardiac (Xu et al., 2015) and neural (Kung et al., 2014) (MuskNeuralink, 2019) (Chung et al., 2019) electrotherapies.

An important limitation for conducting polymers is their relatively poor durability under cyclic electrical, mechanical, and tribological stressing. The gradual loss of the conducting polymer from the substrate often observed after extended implantations *in-vivo* is expected to cause degradation of signal quality and eventual failure (Cui and Zhou, 2007) (Kozai et al., 2015) (Barrese et al., 2016). Ultimately, the failure mode of greatest consequence is film delamination from the substrate.

Attempts to improve film durability have largely involved attempts to stiffen or strengthen the film and/or interface. Carbon-based filler materials (Chen et al., 2000) (Zhang and Zhao, 2012) and crosslinkers (Ouyang et al., 2015) have been used to stiffen and strengthen conducting polymers. Flexible side chains have been added to increase yield and fracture strains (Savagatrup et al., 2014b) (Rodriquez et al., 2017). A number of approaches have been developed to improve the adhesion strength of conjugated polymers to solid substrates. These

<sup>\*</sup> Corresponding author. Materials Science and Engineering, The University of Delaware, Newark, DE, 19716, USA. *E-mail address*: milty@udel.edu (D.C. Martin).

<sup>&</sup>lt;sup>1</sup> Advanced Materials Characterization Lab, 151 Interdisciplinary Science and Engineering Laboratory, University of Delaware, Newark, DE, 19716.

strategies involve both chemical methods intended to increase bond strength (Smela, 1998) (Im et al., 2007) (Sontag et al., 2009) (Carli et al., 2014) (Wei et al., 2015) (Ouyang et al., 2017) and physical methods such as surface roughening to increase the area of adhesive interaction with the substrate (Cui and Martin, 2003) (Green et al., 2012).

Quantifying the effects of these modifications on the most relevant mechanical properties of the polymer has proven difficult due to the challenge of obtaining free-standing films for direct tensile testing. Indirect methods, such as nanoindentation (Yang and Martin, 2006) or AFM indentation (Ouyang et al., 2015) (Hassarati et al., 2014) have been applied to measure the stiffness of these thin films while adhered to a relatively hard, stiff substrate. Direct measurements of mechanical properties such as Young's modulus, yield strength, and strain to failure are possible when substrates are much more compliant than the film (Liu et al., 2015) (Qu et al., 2016). In the buckling method, a film is applied to a pre-stretched polymer substrate; once released, the characteristic wavelength of the wrinkles has been used to extract the modulus of the film based on film thickness and Poisson's ratios of the film and substrate (Davis and Crosby, 2011) (Stafford et al., 2004) (Printz et al., 2015).

Where delamination is concerned, film durability is likely to be at least as sensitive to adhesion strength and interfacial shear strength as it is to the strength and stiffness properties of the film itself. Unfortunately, 'adhesion strength' is poorly defined and difficult to measure. The most common adhesion strength measurements include: (1) scratch testing, which evaluates the critical load at failure (Valli, 1986) (Ollendorf and Schneider, 1999); (2) indentation testing, which creates a blister following debonding (Cordill et al., 2004); (3) peel and pull-off tests (Root et al., 2017), which require a second stronger adhesive interface that does not permeate the film to affect the first; and (4) composite beam bending methods, which directly measure the interfacial shear strength of the bonded interface between elastic members (Root et al., 2017). Each of these common approaches has important limitations with regards to thin, brittle, and possibly permeable films on exposed metallic surfaces.

Raj and Agrawal inspired a new method during theoretical studies of thin film failure mechanics under tensile strains (Agrawal and Raj, 1989) (Agrawal and Raj, 1990). If one strains the substrate in tension, the failed film presents a characteristic crack spacing that only depends on film thickness, film strength, and interfacial shear strength. Tensile strain crack pattern measurements have been used with external measurements of film thickness and strength to quantify the interfacial shear strength for both inorganic (Xie and Tong, 2005) and polymer films (Ye et al., 2015) on metallic substrates. Ye et al. (2015) recently reported that the durability of nominally identical tribologically deposited polytetrafluoroethylene (PTFE)-based films on steel improved by as much as 108 times when they increased frictional energy of deposition beyond a threshold limit. Using tensile strain cracking pattern measurements, they showed that a relatively weaker interface consistently produced films of poor durability while a relatively stronger interface produced films of exceptional durability.

These results support an 'adhesion transition' hypothesis of film removal and suggest that a condition of  $\tau_i/\tau_f>1$  discourages or prevents the delamination mode of polymer film failure. Here, we aim to determine if and how these concepts translate to conducting polymer films in bioelectronics applications. Relative shear strength was varied by applying PEDOT to different substrate conditions and quantified using a validated variant (wire loop method) of the tensile strain cracking pattern method. The films were subjected to tribological and electrical cycling to assess how substrate condition and relative shear strength effect durability. The results demonstrated that changes in the system (i.e. substrate material and surface modifications) can dramatically affect delamination resistance. While both cyclic electrical and tribological testing quickly and severely compromised the PEDOT-substrate interface when  $\tau_i/\tau_f<1$ , neither stimulus caused detectable

interfacial damage when  $\tau_i/\tau_f > 1$ .

#### 2. Experimental procedures

#### 2.1. Materials and preparation

3,4-ethylenedioxythiophene (EDOT), tetrabutyl ammonium perchlorate (TBAP), were purchased from Sigma-Aldrich, and 2,3-dihydrothieno-(3,4-b)(1,4)-dioxine-2-carboxylic acid (EDOT-acid) was purchased from Tractus Chemical. All the chemicals were of analytical grade. Deionized water was from a Millipore Q water purification system. All reagents and solvents were used without further purification, unless otherwise noted. Three substrate conditions were used in this study: untreated stainless steel, EDOT-acid treated stainless steel to improve compatibility with PEDOT, and pure gold. Wire substrates were used for relative shear strength measurements and sheet substrates were used for all other measurements. Soft tempered 304 stainless steel (SS) wires of 508 µm diameter and ~300 nm average surface roughness were purchased from McMaster-Carr; 99.99% pure gold wires of 380 µm diameter and comparable roughness were purchased from Surepure Chemetals. For the electrochemical and mechanical stability tests, 304 SS sheets were purchased from McMaster-Carr (~400 nm average roughness); gold coated glass slides (~50 nm average roughness) were fabricated with magnetron sputtering, the gold coating was sputtered to around 100 nm thick by 30 W DC power with 0.67 nm/s rate under 4.5 mTorr working pressure.

Wire and sheet substrates were ultrasonically cleaned (Kendal HB-23, 220 W) in acetone, 2—propanol, and deionized water, respectively, for 10 min. After drying in a stream of  $\rm N_2$ , the SS wires and sheets were treated in UV Ozone (Novascan PSD UV Ozone cleaner) for 60 min for further cleaning and activation. Half of the SS substrates were dipped into a 10 mM ethanol solution of EDOT-acid at room temperature for 24 h. The substrates were then rinsed with acetonitrile to remove any residual EDOT-acid molecules and finally dried in the air for the electrochemical deposition. More information about the influence EDOT-acid functionalization of inorganic materials, including the effect on surface morphology and wetting properties, was discussed in detail in a previous paper (Wei et al., 2015).

#### 2.2. Fabrication of PEDOT coatings

Electrochemical polymerization was performed with a Gamry Reference 600 Potentiostat/Galvanostat/ZRA and Gamry instruments framework software in a three-electrode cell. PEDOT was polymerized on untreated gold and SS wires, and EDOT-acid treated SS wires under galvanostatic conditions (0.5 mA) from an acetonitrile solution containing 0.02 M EDOT, and 0.1 M TBAP for varying times (from 100 s to 1500 s) to create films of varying thickness (from ~200 nm up to  $\sim$ 7  $\mu$ m). All wires were 20 mm in length, and were coated along the last ~15 mm of their length by dipping the wire into the solution. Electrochemical polymerization on untreated gold coated glass and SS sheets, and EDOT-acid treated SS sheets was performed with the same instrument and software mentioned above, under galvanostatic conditions (0.1 mA) from an acetonitrile solution containing 0.02 M EDOT,  $0.1\,M$  TBAP for  $1000\,s$ . All sheet substrates were 7 mm wide imes 30 mm long, and were coated along the bottom 15 mm, again by controlling the length of electrode in the solution.

#### 2.3. Characterization of relative shear strength

The tensile strain cracking pattern method was used to measure relative shear strength of the PEDOT films for all three substrate conditions. In the standard method, the substrate is strained well-beyond the onset of coating failure. At equilibrium, the failed coating develops a characteristic cracking pattern whose spacing ( $\lambda$ ) only depends on film thickness (t), film shear strength ( $\tau_t$ ), and interfacial shear strength

 $(r_i)$  as first shown theoretically by Raj and Agrawal (Agrawal and Raj, 1989) (Agrawal and Raj, 1990). For the purposes of this study, we use the relative shear strength, defined as the ratio of interfacial and film shear strength. According to the solution from Raj and Agrawal, the relative shear strength is the following function of coating thickness and crack spacing:

$$\tau^* = \frac{2\pi \cdot t}{\lambda} \tag{1}$$

It is worth noting that the solution to this mechanics problem is independent of the stress and strain applied. If the applied strains are too small or if the substrate breaks before the film fails, which will be the case with brittle substrates, no observable cracking pattern will emerge. The characteristic cracking pattern emerges at a critical strain and the distance between stable coating domains of constant width  $\lambda$  simply increases with increased strain; the experimenter knows the necessary experimental conditions have been satisfied when a stable and consistent cracking pattern is observed. These experiments used annealed wires to promote ductility and increase the likelihood of film failure (Qu et al., 2016) (Lang et al., 2009).

Although this method favors ductile substrates, we have found that particularly ductile metals, such as gold, can be problematic due to localized plasticity (i.e. 'necking'). In our preliminary experiments with gold wires, plastic deformation was often localized to a small necking region that prevented the intended measurement. We therefore devised a simple wire loop variant of the method that both prescribed the region of maximum strain and prevented the possibility of necking with ductile substrates. The coated wire was plastically deformed into a loop by wrapping it around a 3 mm diameter mandrel. The mandrel was then removed from the loop and the ends of the wires were pulled by hand in opposing directions to kink the loop at the apex where the moment, stress, and strain were maximized (Fig. 1c). The average crack spacing and coating thickness were measured at multiple domains in the vicinity of the apex with a Zeiss Auriga 60 Focused Ion Beam-Scanning Electron Microscope (FIB-SEM) operating at 3 kV. A representative SEM image of a coating on an untreated stainless steel wire following wire

loop testing is shown in Fig. 1d. We used the SEM to quantify crack spacing and thickness at the single domain on samples of varying thickness at each substrate condition; N>6 independent measurements of crack spacing and thickness were made for each sample. A linear regression of mean crack spacing and thickness was used with Eq. (1) to determine relative shear strength of nominally identical systems of varying thickness; a Monte Carlo method was used to determine the experimental uncertainty in relative shear strength following the approach from Burris and Sawyer (2009). Comparing the results from the wire loop method to those of the standard tensile testing method using PEDOT on stainless steel revealed no statistically significant effect from the wire loop modification (Fig. 3f).

#### 2.4. Characterization of electrochemical stability

The PEDOT coated substrates were scanned from +0.8~V to -0.8~V for 3000 cycles in PBS (1x), with 100 mV/s scan rate. The PEDOT coated substrates (untreated SS, treated SS, and Au sheets) were used as the working electrodes, with a  $10~mm \times 10~mm$  platinum sheet counter electrode, and a Ag/AgCl reference electrode. The morphology of the PEDOT of pristine and scanned samples was observed in a Zeiss Auriga 60 FIB/SEM at 3~kV.

#### 2.5. Characterization of mechanical stability

A custom *in-situ* linear reciprocating tribometer (illustrated in Fig. 2.) was used to mimic the sliding behavior between the coated electrodes and the soft tissues typical of the bioelectronics applications of interest. The normal and friction forces were determined using capacitive displacements sensors to measure normal and transverse deflections of the pre-calibrated loading beam as described elsewhere (Bonnevie et al., 2011) (Moore and Burris, 2014). For this study, fresh room temperature pork loin was chosen as the counterbody because of its clinical relevance as a model muscle tissue. Each 4–5 mm diameter cylinder of muscle was attached to the loading beam with

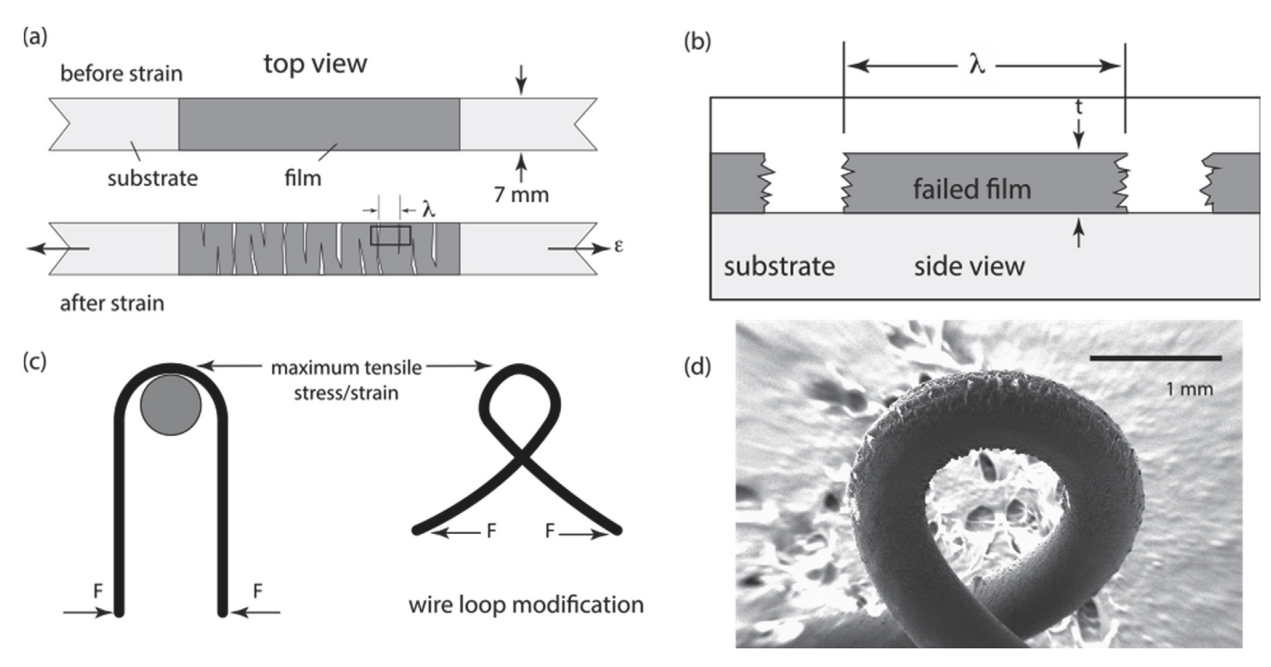


Fig. 1. Illustrations of the tensile strain cracking pattern method (a and b) and the wire loop modification (c) used to characterize relative shear strength of PEDOT films on varying substrates. (a) Top-down view of the standard strain test. (b) Side view of the test illustrating a point-wise measurement of crack spacing ( $\lambda$ ) and coating thickness (t) at a single 'domain' of failed film. (c) Schematic of the wire loop modification. Under any pulling force, F, the maximum moment occurs at the apex of the loop. (d) SEM image of a representative sample following the wire loop pull test. Unlike the tensile test, in which local plastic instabilities (necking) of ductile substrates can destroy the measurement, the wire loop version of the test guarantees the location of maximum tensile strain on the outside and at the apex of the wire loop as shown.

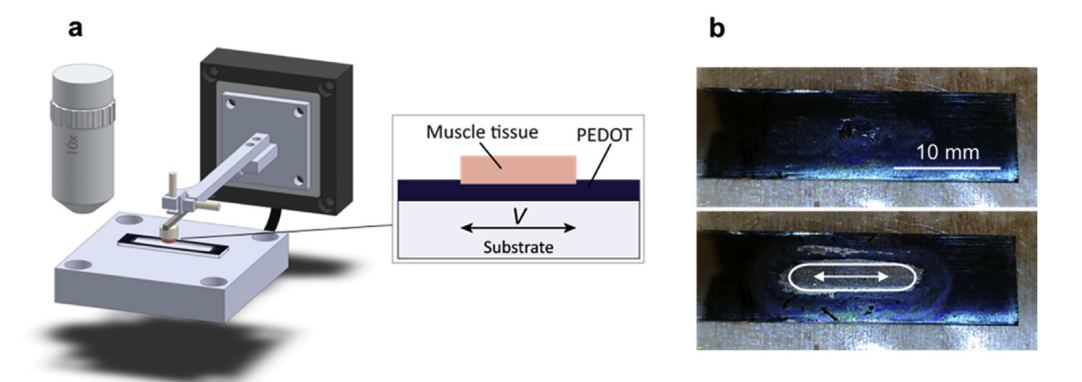


Fig. 2. (a) The experimental setup for tribological durability testing: porcine loin muscle was attached to the loading beam and rubbed against PEDOT coating deposited on different substrates and surface treatments. (b) Optical images of a PEDOT coating on untreated SS substrate during the wear test after cycles 1 and 50.

cyanoacrylate adhesive and loaded to 20 mN to achieve a target contact pressure of 1–1.6 kPa, which approximates the fluid pressure of lower limbs (range -1 to 10 mmHg (Olszewski et al., 2010)). The muscle tissue slid against the coating over a 10 mm long track at a fixed nominal speed of 5 mm/s.

Damage was quantified by periodically interrupting the test and taking *in-situ* optical microscopy images of the worn region. ImageJ software was used to determine the area removed by sliding as shown. The area removed was quantified after  $N=0,\,1,\,2,\,5,\,10,\,20,\,50,\,100,$  and 200 cycles. The fraction of lost surface area ratio was determined by A/A<sub>t</sub>, where A is the lost surface area, and A<sub>t</sub> is the total wear track area.

#### 3. Results

#### 3.1. Relative shear strength

SEM images of the cracked PEDOT film at the apex of representative wire loop tests are shown in Fig. 3a-c at the same magnification; for a given material system with constant film thickness, decreased crack spacing reflects increased relative shear strength. The quantified crack spacing is plotted as a function of measured coating thickness for each of the three substrate conditions in Fig. 3d. Against stainless steel, the PEDOT film had a crack spacing per unit thickness of  $35.1 \pm 3.7$ , which corresponds to a relative shear strength of  $0.18 \pm 0.02$  (Fig. 3f); in other words, the interface was less than 20% the strength of the film on average. The EDOT-acid surface treatment improved the interfacial

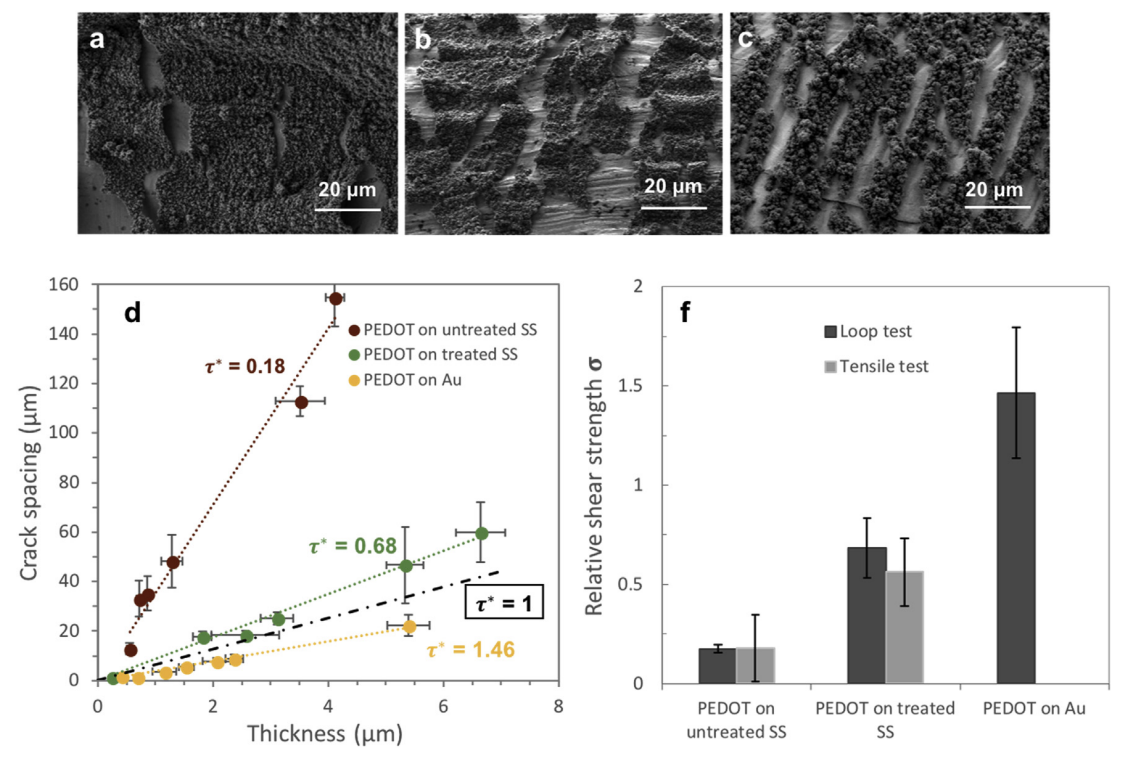


Fig. 3. SEM images of PEDOT film cracking: (a) PEDOT film ( $\sim$ 0.8  $\mu$ m thick) on untreated SS, (b) PEDOT film ( $\sim$ 1  $\mu$ m thick) on treated SS, and (c) PEDOT film ( $\sim$ 2  $\mu$ m thick) on Au. (d) The statistics of crack spacing vs. thickness of PEDOT on 3 different substrates from the loop test ( $\tau^* = \tau_i/\tau_f$ ). (f) The statistics of the relative shear strength from loop and tensile tests (tensile tests on gold resulted in necking and ultimate failure rather than uniform plastic deformation – this inspired the use of a loop test). (For interpretation of the references to colour in this figure legend, the reader is referred to the Web version of this article.)

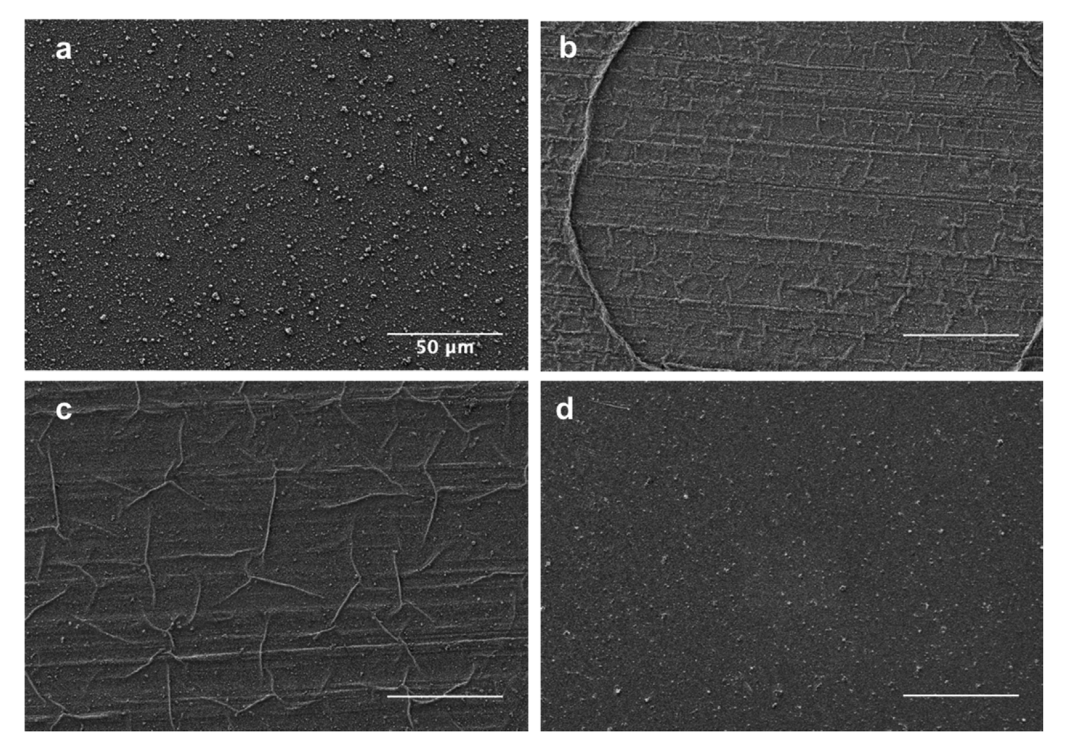


Fig. 4. SEM images before and after CV test: (a) PEDOT surface before CV test. (b) PEDOT on untreated SS after CV test, with a large circular wrinkle and many smaller wrinkles. (c) PEDOT on treated SS after CV, with fewer wrinkles. (d) PEDOT on Au after CV, with no wrinkles. Scale bars are 50 µm.

shear strength of the PEDOT film; crack spacing per unit thickness decreased to 9.1  $\pm$  2.0, which corresponds to a relative shear strength of 0.69  $\pm$  0.15. PEDOT had the greatest interfacial strength on pure untreated gold. In this case, the crack spacing per unit thickness decreased to 4.3  $\pm$  1.0 and the relative shear strength increased to 1.46  $\pm$  0.33. Against gold, the bonded interface is actually stronger than the film itself and, based on the adhesion transition hypothesis, one would expect PEDOT on gold to be substantially more durable than PEDOT on treated or untreated stainless steel.

#### 3.2. Electrochemical stability and the potential of PEDOT failure

Before the electrochemical stability (CV) testing, there were no obvious differences in the visual appearance of the PEDOT films under the 3 substrate conditions of this study (Fig. 4a). In the case of the untreated stainless steel, 3000 cycles of CV scanning led to significant film wrinkling (Fig. 4b), which suggest that repeated swelling and shrinking during redox switching compromised the integrity of the adhesive interface. EDOT-acid treatment altered the qualitative appearance of the wrinkling following CV scanning, but it did not prevent interface damage (Fig. 4C). Conversely, CV scanning on PEDOT-gold caused no obvious visual evidence of interfacial or surface degradation (Fig. 4d).

### 3.3. Mechanical stability and the potential degradation of signal transfer performance

PEDOT coated surfaces were slid at low pressure against pork loin to determine if and how the relative shear strength affects resistance to tribological stresses. The percentage of total film area removed is plotted as a function of distance slid in Fig. 5. Against untreated stainless steel, ~25% of the PEDOT film was removed on the first sliding cycle. Against treated stainless steel, the PEDOT film endured 20–40 sliding cycles prior to any significant removal of material. Against Au, we observed no evidence of material removal across the

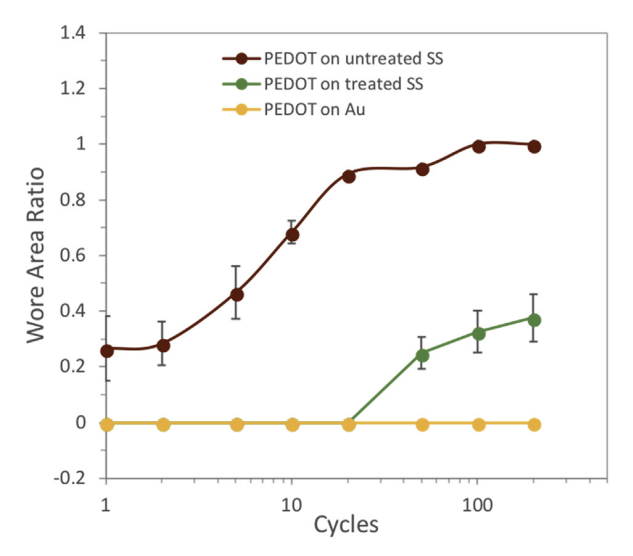


Fig. 5. Lost area ratio as a function of the number cycles during wear testing.

length of the 200 cycle test. Furthermore, no damage was observed after an additional 500 sliding cycles. These results suggest that mechanical failure is extremely sensitive to relative shear strength and are consistent with the adhesion transition hypothesis of film failure.

#### 4. Discussion

Mechanical durability, and delamination in particular, of conducting polymers on inorganic substrates is a significant technical challenge in a number of areas including bioelectronics. Many attempts have been made to resolve this issue using materials design and chemistry-based approaches to increase strength and toughness of the film and the bonded interface. In this paper, we demonstrate that

Table 1
Relative shear strength and durability of PEDOT on different substrates.

	Relative shear strength	Tribological failure cycles	Interface integrity after CV scans
Untreated SS	0.18	1–2	Significant wrinkling
Treated SS	0.69	20–30	Wrinkling
Au	1.46	> 500	No wrinkle

changes in substrate conditions can significantly improve interfacial properties of the film. Moreover, we show that increased relative shear strength  $(\tau_i/\tau_f)$  to beyond 1 radically improves failure resistance under mechanical and electrical cycling (see Table 1)

The results provide no direct insight into whether the improvements in relative shear strength reported here are due to increased interfacial shear strength, decreased film strength, or a combination of the two. It seems unlikely that altering the substrate metal would significantly reduce the bulk strength of the film. The most intuitive interpretation is that PEDOT on gold had significantly improved interfacial shear strength, which caused increased relative shear strength and durability. While we did not attempt to measure interfacial shear strength directly, we can infer its magnitude if we assume bulk PEDOT properties from the literature ( $\sigma = 56 \, \text{MPa}$  (Qu et al., 2016)); on this basis, our direct measurements of relative shear strength suggest that the interfacial shear strength of the PEDOT film was 5.0 MPa, 19 MPa, and 41 MPa against untreated stainless steel, EDOT-acid treated stainless steel, and Au, respectively.

The concept of relative shear strength provides some important insights into the unusually strong effects observed in this study. Against untreated stainless steel, the interfacial shear strength was about 20% the shear strength of PEDOT. This is reasonable for incompatible materials linked primarily through physical interactions. It is also reasonable to expect an EDOT-acid surface treatment designed to improve interfacial compatibility to also improve interfacial shear strength by > 200%; in this case, the interface was still less than 80% the strength of the film itself. The PEDOT-Au interface was 46% stronger than the PEDOT film, which indicates that the interactions between polymer chains and gold were stronger than those between polymer chains. Previous results from X-ray photoelectron spectroscopy studies of this system (Terzi et al., 2011) (Samba, 2013) are consistent with strong chemical interactions between the Au and S in the thiophenes. Such an interaction may help explain the strong PEDOT-Au interface observed here.

Aside from the engineering challenges of improving and quantifying interfacial strength, key scientific questions remain about how film and interface strength and toughness affect system durability. One interesting observation from this study is the strongly nonlinear relationship between interfacial strength and durability. A 3.8 times increase in relative shear strength (0.18-0.69) from EDOT-acid treatment of stainless steel only modestly improved tribological durability but an additional 2.1 times increase in shear strength for PEDOT against Au prevented interfacial damage during tribological and electrical testing altogether. According to the adhesion-transition hypothesis, the weak interface limits traction stresses and thereby protects all stronger interfaces. By definition, failure can only occur within the film or at the tribological interface when  $(\tau_i/\tau_f > 1)$ . Thus, unlike interfacial shear strength, the relative shear strength may be an independent predictor of film durability and its transition value is theoretically defined as 1. It is worth mentioning that a mean relative shear strength above 1 is insufficient to ensure a robust film since statistical variations (see Fig. 3d) can create domains of a relative weak bonded interface. The interface will only be robust if  $\tau_i/\tau_f > 1$  everywhere. In this case, a mean relative shear strength of 1.5 was sufficiently larger than the critical value to accommodate any such statistical variations.

The highly nonlinear relationship between interfacial shear strength

and film failure rates, the interfacial shear strength required to prevent damage ( $\sim$ 20 MPa), and the relative shear strength required to prevent damage ( $\sim$ 1.5) observed here are all consistent with previous observations from Ye et al. (2015). The generality suggested by these studies provides the materials designer with powerful new tools: (1) the relative shear strength appears to be a system-insensitive predictor of film durability; (2) relative shear strength can be assessed easily and directly for a wide range of metallic substrates with the wire loop modified tensile strain crack pattern method.

The following limitations should be kept in mind. First, the wire loop method used herein departs from the model situation for which the theoretical solution was developed (Martin, 2003). One obvious difference is the small twist angle from looping. This can be overcome with a crimped 'U' and other possible arrangements but results of validation testing against the standard tensile test (Fig. 3f) alleviated our concerns over these differences. Additionally, because we were more concerned about creating differences in interface properties than the causes of those differences, we made no attempts to control parameters known to affect interfacial strength such as surface energy and roughness. For example, the gold substrate for tribological and electrical testing was sputtered onto smooth glass, whereas wire loop tests were conducted on pure gold wires that were an order of magnitude rougher. It is possible, if not likely, that surface topography, contamination, oxides, substrate strength, and other factors contributed to differences in interfacial shear strength.

#### 5. Conclusions

There are three important conclusions from this study. First, the simple yet robust method developed to quantify the relative shear strength of PEDOT on ductile metallic substrates is widely applicable for multiple deposition methods, such as electrochemical, chemical, and vapor phase depositions, of diverse conducting polymer films. This method can be also extended to the systems with polymer substrates, but not limited to the metallic substrates. Second, quantifying the effect of substrate and surface treatment on the relative shear strength of PEDOT films has provided insights for substrate modification and material selection. Third, changes in relative shear strength to resistance to interface failure under cyclic electrical and tribological testing have been correlated, confirming the utility of the relative shear strength as a measure of durability. Treating stainless steel substrates with an adhesion promoter increased relative shear strength of PEDOT films from 0.18 to 0.69. On untreated gold, the relative shear strength of PEDOT increased to 1.46; i.e. the bonded interface on gold was significantly stronger than the film. Whereas both cyclic electrical and tribological testing quickly and severely damaged the PEDOT/substrate interface when the relative shear strength  $(\tau_i/\tau_f)$  was less than 1, neither stimulus damaged the interface when the relative shear strength  $(\tau_i/\tau_f)$  exceeded

#### **Funding**

This work was supported in part by the Defense Advanced Research Projects Agency grant N66001- 11-C-4190, the National Institutes of Health EUREKA grant 1RO1EB010892, the National Science Foundation (DMR-1505144 and DMR-1808048), and by the University of Delaware.

#### Acknowledgements

We acknowledge the Department of Physics (Dr. Tao Wang and Prof. John Xiao) at the University of Delaware for the use of their Magnetron sputtering system.

#### References

- Agrawal, D., Raj, R., 1989. Measurement of the ultimate shear strength of a metal-ceramic interface. Acta Metall. 37, 1265–1270. https://doi.org/10.1016/0001-6160(89) 90120-X.
- Agrawal, D., Raj, R., 1990. Ultimate shear strengths of copper-silica and nickel-silica interfaces. Mater. Sci. Eng. A 126, 125–131.
- Barrese, J.C., Aceros, J., Donoghue, J.P., 2016. Scanning electron microscopy of chronically implanted intracortical microelectrode arrays in non-human primates. J. Neural Eng. 13. 026003. https://doi.org/10.1088/1741-2560/13/2/026003.
- Berggren, M., Richter-Dahlfors, A., 2007. Organic bioelectronics. Adv. Mater. 19, 3201–3213. https://doi.org/10.1002/adma.200700419.
- Bodart, C., Rossetti, N., Hagler, J., Chevreau, P., Chhin, D., Soavi, F., Schougaard, S.B., Amzica, F., Cicoira, F., 2019. Electropolymerized poly(3,4-ethylenedioxythiophene) (PEDOT) coatings for implantable deep-brain-stimulating microelectrodes. ACS Appl. Mater. Interfaces 11, 17226–17233. https://doi.org/10.1021/acsami.9b03088.
- Boehler, C., Oberueber, F., Schlabach, S., Stieglitz, T., Asplund, M., 2016. Long-term stable adhesion for conducting polymers in biomedical applications: IrOx and nanostructured platinum solve the chronic challenge. ACS Appl. Mater. Interfaces 9, 189–197. https://doi.org/10.1021/acsami.6b13468.
- Bonnevie, E.D., Baro, V.J., Wang, L., Burris, D.L., 2011. In situ studies of cartilage microtribology: roles of speed and contact area. Tribol. Lett. 41, 83–95. https://doi.org/10.1007/s11249-010-9687-0.
- Burris, D.L., Sawyer, W.G., 2009. Measurement uncertainties in wear rates. Tribol. Lett. 36, 81–87. https://doi.org/10.1007/s11249-009-9477-8.
- Carli, S., Casarin, L., Bergamini, G., Caramori, S., Bignozzi, C.A., 2014. Conductive PEDOT covalently bound to transparent FTO electrodes. J. Phys. Chem. C 118, 16782–16790. https://doi.org/10.1021/jp412758g.
- Chen, G.Z., Shaffer, M.S.P., Coleby, D., Dixon, G., Zhou, W., Fray, D.J., Windle, A.H., 2000. Carbon nanotube and polypyrrole composites: coating and doping. Adv. Mater. 12, 522–526. https://doi.org/10.1002/(SICI)1521-4095(200004)12:7 < 522::AID-ADMA522 > 3.0.CO;2-S.
- Chen, R., Canales, A., Anikeeva, P., 2017. Neural recording and modulation technologies. Nat. Rev. Mater. 2, 16093. https://doi.org/10.1038/natrevmats.2016.93.
- Chung, J.E., Joo, H.R., Fan, J.L., Liu, D.F., Barnett, A.H., Chen, S., Geaghan-Breiner, C., Karlsson, M.P., Karlsson, M., Lee, K.Y., Liang, H., Magland, J.F., Pebbles, J.A., Tooker, A.C., Greengard, L.F., Tolosa, V.M., Frank, L.M., 2019. High-density, long-lasting, and multi-region electrophysiological recordings using polymer electrode arrays. Neuron 101, 21–31. https://doi.org/10.1016/j.neuron.2018.11.002.e5
- 101, 21–31. https://doi.org/10.1016/j.neuron.2018.11.002. e5.
  Cordill, M.J., Bahr, D.F., Moody, N.R., Gerberich, W.W., 2004. Recent developments in thin film adhesion measurement. IEEE Trans. Device Mater. Reliab. 4, 163–168. https://doi.org/10.1109/TDMR.2004.829071.
- Cui, X., Martin, D.C., 2003. Fuzzy gold electrodes for lowering impedance and improving adhesion with electrodeposited conducting polymer films. Sens. Actuators A Phys. 103, 384–394. https://doi.org/10.1016/S0924-4247(02)00427-2.
- Cui, X.T., Zhou, D.D., 2007. Poly (3,4-ethylenedioxythiophene) for chronic neural stimulation. IEEE Trans. Neural Syst. Rehabil. Eng. 15, 502–508. https://doi.org/10.1097/00004691-198701000-00012.
- Davis, C.S., Crosby, A.J., 2011. Mechanics of wrinkled surface adhesion. Soft Matter 7 (11), 5373. https://doi.org/10.1039/c1sm05146f.
- Forrest, S.R., 2004. The path to ubiquitous and low-cost organic electronic appliances on plastic. Nature 428, 911–918.
- Green, R.a., Hassarati, R.T., Bouchinet, L., Lee, C.S., Cheong, G.L.M., Yu, J.F., Dodds, C.W., Suaning, G.J., Poole-Warren, L.a., Lovell, N.H., 2012. Substrate dependent stability of conducting polymer coatings on medical electrodes. Biomaterials 33, 5875–5886. https://doi.org/10.1016/j.biomaterials.2012.05.017.
- Hassarati, R.T., Goding, J.a., Baek, S., Patton, A.J., Poole-Warren, L.a., Green, R.a., 2014. Stiffness quantification of conductive polymers for bioelectrodes. J. Polym. Sci., Part B: Polym. Phys. 52, 666–675. https://doi.org/10.1002/polb.23465.
- Im, S.G., Yoo, P.J., Hammond, P.T., Gleason, K.K., 2007. Grafted conducting polymer films for nano-patterning onto various organic and inorganic substrates by oxidative chemical vapor deposition. Adv. Mater. 19, 2863–2867. https://doi.org/10.1002/ adma.200701170.
- Kozai, T.D.Y., Catt, K., Li, X., Gugel, Z.V., Olafsson, V.T., Vazquez, A.L., Cui, X.T., 2015. Mechanical failure modes of chronically implanted planar silicon-based neural probes for laminar recording. Biomaterials 37, 25–39. https://doi.org/10.1016/j. biomaterials.2014.10.040.
- Kung, T., Langhals, N., Martin, D., Johnson, P., Cederna, P., Urbanchek, M., 2014. Regenerative peripheral nerve interface viability and signal transduction with an implanted electrode. Plast. Reconstr. Surg. 133, 1380–1394. https://doi.org/10. 1097/PRS.000000000000168.
- Lang, U., Naujoks, N., Dual, J., 2009. Mechanical characterization of PEDOT:PSS thin films. Synth. Met. 159, 473–479. https://doi.org/10.1016/j.synthmet.2008.11.005.
- Lee, H., V Bellamkonda, R., Sun, W., Levenston, M.E., 2005. Biomechanical analysis of silicon microelectrode-induced strain in the brain. J. Neural Eng. 2, 81–89. https:// doi.org/10.1088/1741-2560/2/4/003.
- Leleux, P., Johnson, C., Strakosas, X., Rivnay, J., Hervé, T., Owens, R.M., Malliaras, G.G., 2014. Ionic liquid gel-assisted electrodes for long-term cutaneous recordings. Adv. Healthc. Mater. 3, 1377–1380. https://doi.org/10.1002/adhm.201300614.
- Lind, G., Linsmeier, C.E., Schouenborg, J., 2013. The density difference between tissue and neural probes is a key factor for glial scarring. Sci. Rep. 3, 2942. https://doi.org/ 10.1038/srep02942.
- Liu, Y., Chen, Y.C., Hutchens, S., Lawrence, J., Emrick, T., Crosby, A.J., 2015. Directly measuring the complete stress-strain response of ultrathin polymer films. Macromolecules 48, 6534–6540. https://doi.org/10.1021/acs.macromol.5b01473.

- Martin, D.C., 2003. Elastica bend testing of the effective interfacial shear strength and critical deformation strains of brittle coatings on ductile substrates. Prog. Org. Coat. 48, 332–336. https://doi.org/10.1016/j.porgcoat.2002.11.001.
- Moore, A.C., Burris, D.L., 2014. An analytical model to predict interstitial lubrication of cartilage in migrating contact areas. J. Biomech. 47, 148–153. https://doi.org/10. 1016/j.jbiomech.2013.09.020.
- Musk, E., Neuralink, 2019. An Integrated Brain-Machine Interface Platform with Thousands of Channels. BioRxiv, pp. 703801. https://doi.org/10.1101/703801.
- Nyberg, T., Shimada, A., Torimitsu, K., 2007. Ion conducting polymer microelectrodes for interfacing with neural networks. J. Neurosci. Methods 160, 16–25. https://doi.org/ 10.1016/j.ineumeth.2006.08.008.
- Ollendorf, H., Schneider, D., 1999. A comparative study of adhesion test methods for hard coatings. Surf. Coat. Technol. 113, 86–102. https://doi.org/10.1016/S0257-8977(98)00827.5
- Olszewski, W.L., Jain, P., Ambujam, G., Zaleska, M., Cakala, M., Gradalski, T., 2010. Tissue fluid pressure and flow in the subcutaneous tissue in lymphedema - hints for manual and pneumatic compression therapy. Phlebolymphology 17, 144–150.
- Ouyang, L., Kuo, C., Farrell, B., Pathak, S., Wei, B., Qu, J., Martin, D.C., 2015. Poly[3,4-ethylene dioxythiophene (EDOT)-co-1,3,5-tri[2-(3,4-ethylene dioxythienyl)]-benzene (EPh)] copolymers (PEDOT-co-EPh): optical, electrochemical and mechanical properties. J. Mater. Chem. B. 00, 1–11. https://doi.org/10.1039/CSTB000531.
- Ouyang, L., Wei, B., Kuo, C., Pathak, S., Farrell, B., Martin, D.C., 2017. Enhanced PEDOT adhesion on solid substrates with electrografted P(EDOT-NH2). Sci. Adv. 3. https://doi.org/10.1126/sciadv.1600448.
- Printz, A.D., Zaretski, A.V., Savagatrup, S., Chiang, A.S.C., Lipomi, D.J., 2015. Yield point of semiconducting polymer films on stretchable substrates determined by onset of buckling. ACS Appl. Mater. Interfaces 7, 23257–23264. https://doi.org/10.1021/ acsami\_5b08628
- Qu, J., Ouyang, L., Kuo, C.C., Martin, D.C., 2016. Stiffness, strength and adhesion characterization of electrochemically deposited conjugated polymer films. Acta Biomater. 31, 114–121. https://doi.org/10.1016/j.actbio.2015.11.018.
- Rodriquez, D., Kim, J.-H., Root, S.E., Fei, Z., Boufflet, P., Heeney, M., Kim, T.-S., Lipomi, D.J., 2017. Comparison of methods for determining the mechanical properties of semiconducting polymer films for stretchable electronics. ACS Appl. Mater. Interfaces 9, 8855–8862. https://doi.org/10.1021/acsami.6b16115.
- Root, S.E., Savagatrup, S., Printz, A.D., Rodriquez, D., Lipomi, D.J., 2017. Mechanical properties of organic semiconductors for stretchable, highly flexible, and mechanically robust electronics. Chem. Rev. 117, 6467–6499. https://doi.org/10.1021/acs. chemrev.7b00003.
- Samba, R., 2013. Is the enhanced adhesion of PEDOT thin films on electrodes due to sulfur - gold interaction? - an XPS study. Open Surf. Sci. J. 5, 17–20. https://doi.org/ 10.2174/1876531901305010017.
- Savagatrup, S., Printz, A.D., O'Connor, T.F., Zaretski, A.V., Lipomi, D.J., 2014a. Molecularly stretchable electronics. Chem. Mater. 26, 3028–3041. https://doi.org/ 10.1021/cm501021v.
- Savagatrup, S., Makaram, A.S., Burke, D.J., Lipomi, D.J., 2014b. Mechanical properties of conjugated polymers and polymer-fullerene composites as a function of molecular structure. Adv. Funct. Mater. 24, 1169–1181. https://doi.org/10.1002/adfm. 20130346
- Sessolo, M., Khodagholy, D., Rivnay, J., Maddalena, F., Gleyzes, M., Steidl, E., Buisson, B., Malliaras, G.G., 2013. Easy-to-Fabricate conducting polymer microelectrode arrays. Adv. Mater. 2135–2139. https://doi.org/10.1002/adma.201204322.
- Smela, E., 1998. Thiol-modified pyrrole monomers: 4. Electrochemical deposition of polypyrrole over 1-(2-thioethyl)pyrrole. Langmuir 14, 2996–3002. https://doi.org/ 10.1021/la970863e.
- Someya, T., Bao, Z., Malliaras, G.G., 2016. The rise of plastic bioelectronics. Nature 540, 379–385. https://doi.org/10.1038/nature21004.
- Sontag, S.K., Marshall, N., Locklin, J., 2009. Formation of conjugated polymer brushes by surface-initiated catalyst-transfer polycondensation. Chem. Commun. 3354–3356. https://doi.org/10.1039/b907264k.
- Stafford, C.M., Harrison, C., Beers, K.L., Karim, A., Amis, E.J., VanLandingham, M.R., Kim, H.C., Volksen, W., Miller, R.D., Simonyi, E.E., 2004. A buckling-based metrology for measuring the elastic moduli of polymeric thin films. Nat. Mater. 3, 545–550. https://doi.org/10.1038/nmat1175.
- Terzi, F., Pasquall, L., Montecchi, M., Nannarone, S., Viinikanoja, A., Ääritalo, T., Salomäki, M., Lukkari, J., Doyle, B.P., Seeber, R., 2011. New insights on the interaction between thiophene derivatives and Au surfaces. the case of 3,4-ethylene-dioxythiophene and the relevant polymer. J. Phys. Chem. C 115, 17836–17844. https://doi.org/10.1021/jp203219b.
- Valli, J., 1986. A review of adhesion test methods for thin hard coatings. J. Vac. Sci. Technol. A Vacuum, Surfaces, Film. 4, 3007. https://doi.org/10.1116/1.573616.
- Venkatraman, S., Hendricks, J., a King, Z., Sereno, A.J., Richardson-Burns, S., Martin, D., Carmena, J.M., 2011. In vitro and in vivo evaluation of PEDOT microelectrodes for neural stimulation and recording. IEEE Trans. Neural Syst. Rehabil. Eng. 19, 307–316. https://doi.org/10.1109/TNSRE.2011.2109399.
- Wei, B., Liu, J., Ouyang, L., Kuo, C.-C., Martin, D.C., 2015. Significant enhancement of PEDOT thin film adhesion to inorganic solid substrates with EDOT-acid. ACS Appl. Mater. Interfaces 7, 15388–15394. https://doi.org/10.1021/acsami.5b03350.
- Wilks, S.J., Richardson-Burns, S.M., Hendricks, J.L., Martin, D.C., Otto, K.J., 2009. Poly (3,4-ethylenedioxythiophene) as a micro-neural interface material for electrostimulation. Front. Neuroeng. 2, 7. https://doi.org/10.3389/neuro.16.007.2009.
- Xie, C., Tong, W., 2005. Cracking and decohesion of a thin Al2O3 film on a ductile Al-5% Mg substrate. Acta Mater. 53, 477–485. https://doi.org/10.1016/j.actamat.2004.10. 005
- Xu, L., Gutbrod, S.R., Ma, Y., Petrossians, A., Liu, Y., Webb, R.C., Fan, J.A., Yang, Z., Xu, R., Whalen, J.J., Weiland, J.D., Huang, Y., Efimov, I.R., Rogers, J.A., 2015. Materials

- and fractal designs for 3D multifunctional integumentary membranes with capabilities in cardiac electrotherapy. Adv. Mater. 27, 1731–1737. https://doi.org/10.1002/adma.201405017
- Yang, J., Martin, D.C.D., 2006. Impedance spectroscopy and nanoindentation of conducting poly(3,4-ethylenedioxythiophene) coatings on microfabricated neural prosthetic devices. J. Mater. Res. 21, 1124–1132. https://doi.org/10.1557/jmr.2006.
- Ye, J., Moore, A.C., Burris, D.L., 2015. Transfer film tenacity: a case study using ultra-low-wear alumina-PTFE. Tribol. Lett. 59, 1–11. https://doi.org/10.1007/s11249-015-0576-4
- Zhang, J., Zhao, X.S., 2012. Conducting polymers directly coated on reduced graphene oxide sheets as high-performance supercapacitor electrodes. J. Phys. Chem. C 116, 5420–5426. https://doi.org/10.1021/jp211474e.